GE HealthCare

White Paper

Supercharge Spectral CT with TrueFidelity for Gemstone Spectral Imaging (GSI)

The Peer-Reviewed Evidence Summary of Deep Learning Image Reconstruction for GSI

Hugo Pasquier, Ph.D. and Eugene Huayang Liu, M.D.

Contents

Abstract

Spectral CT has emerged to be a powerful radiological evaluation tool, with proven benefits in improving image quality and lesion detectability, while at the same time optimizing radiation and contrast media doses.

To enhance its clinical adoption and diagnostic value, GE HealthCare, a pioneer in Spectral CT innovations, introduced TrueFidelity for GSI, a breakthrough deep learning image reconstruction solution for CT spectral imaging.

This white paper summarizes recently released peer-reviewed evidence to demonstrate how TrueFidelity for GSI supercharges spectral CT by elevating image quality and diagnostic performance.

Background

Spectral Computed Tomography (CT), also referred to as Dual Energy CT (DECT), acquires projections at two energy spectra. It allows the differentiation and classification of different tissues based on differences in photon absorption. Via material decomposition algorithms, various spectral CT image types can be generated, including virtual monochromatic (also known as keV), material-selective and virtual unenhanced (VUE) images. These images have been proven to improve contrast-to-noise ratio (CNR) and aid in detecting and characterizing lesions, minimizing noise, and reducing artifacts.[1]

GE HealthCare (GEHC) has pioneered Spectral CT with Gemstone Spectral Imaging (GSI) that employs ultra-fast kV switching during dual energy data acquisition: the x-ray source switches rapidly between 80 kVp and 140 kVp at sub-millisecond speed, producing nearly simultaneous dual energy projections at the same orientation to minimize the impacts of patient and organ motion, and without the compromise of maximum 50cm scan field of view and fast acquisition speed.[2]

Since being introduced in 2010, innovations have been developed to enhance GSI's clinical adoption (Figure 1). This allows GSI users worldwide to explore its diagnostic value in a wide range of clinical applications from neurology, oncology, pulmonology, cardiovascular, musculoskeletal, to even emergency medicine.

Table 1 summarizes GSI diagnostic value in various indications based on selected publications.

As shown in table 1, two GSI image types are playing critical roles in enhancing lesion detection and characterization: low-energy keV images and material-specific iodine images. The use of keV images of a lower energy level (40–70 keV) may improve iodine conspicuity and lesion-to-background contrast, thus, improving lesion detectability. Material-specific iodine images help with lesion characterization by enabling differentiation of hypo-attenuating tumors from hypo- or hyper-attenuating cysts, and facilitate detection of iso-attenuating tumors, such as pancreatic masses and peritoneal disease. Moreover, quantitative iodine mapping may serve as a surrogate biomarker for treatment planning and monitoring.

Spectral CT has been proven to improve contrast-to-noise ratio and aid in detecting and characterizing lesions, minimizing noise, and reducing artifacts.[1]

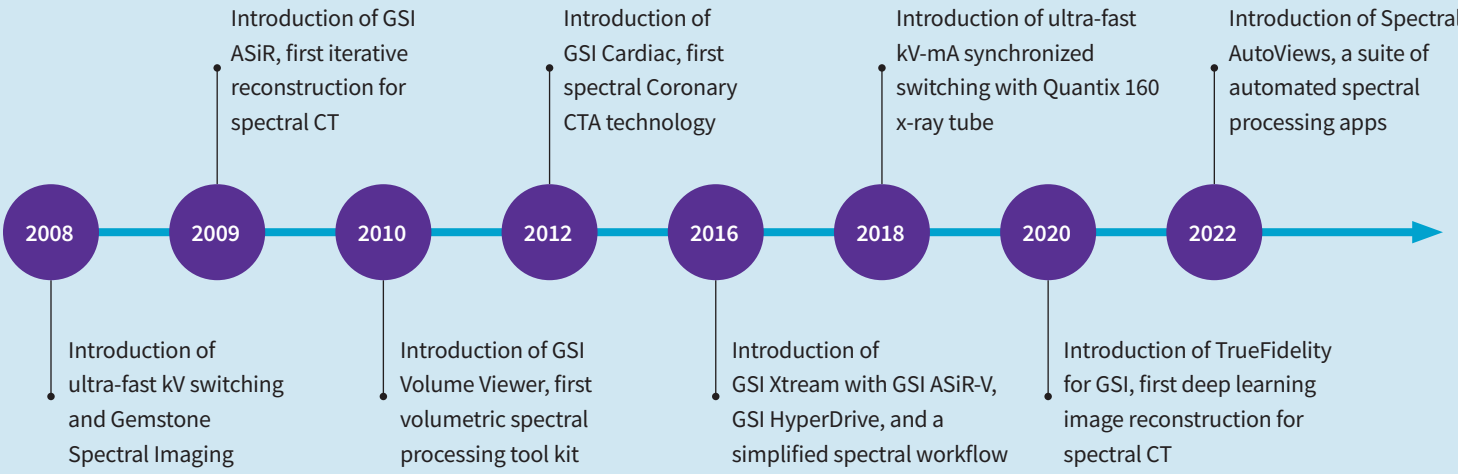

Figure 1: GEHC's innovation timeline on spectral CT.
ASiR denotes Adaptive Statistical Iterative Reconstruction, ASiR-V Adaptive Statistical Iterative Reconstruction - V.

Table 1: Summary of clinical studies that evaluated GSI's application and benefits in different clinical indications.

Anatomy	Indication	Patient cohort	Diagnostic value	Citation	Reference
Head	Acute ischemic stroke	42	Tissue characterization	The iodine concentration of ischemic penumbral area derived from pre-treatment spectral CT angiography was an independent predictor of hemorrhagic transformation after intravenous thrombolysis treatment for acute ischemic stroke patients.	3
Head and Neck	Squamous Cell Carcinoma	60	Lesion Detection	Low energy virtual monochromatic images improve tumor visibility objectively and subjectively both by head and neck specialists and general radiologists.	4
Chest	Lung cancer	77	Tissue characterization	GSI technique might be helpful to differentiate lung cancer from lung benign lesions by providing qualitative and quantitative information.	5
Chest	Lung cancer	32	Tissue characterization	Iodine quantification using GSI is feasible and can quantitatively evaluate pulmonary perfusion and identify perfusion defects that are induced by central lung cancer.	6
Cardiac	Coronary CT Angiography	67	Improved diagnostic performance	Calcium-suppressed iodine material density images reduced false-positive and increased the diagnostic performance for calcified coronary artery lesions compared to conventional CCTA images.	7
Cardiac	Transcatheter Aortic Valve Implantation	21	Tissue characterization/ treatment planning	Extracellular volume measurement based on iodine map from an additional spectral CT acquisition in TAVI planning may determine its prognostic significance.	8
Liver	Hepatocellular Carcinoma	30	Lesion detection and tissue characterization	Low keV monochromatic and iodine(water) images could significantly improve the detection and characterization of multiple lesions, assess tumor homogeneity and identify residual, recurrent or metastatic lesions during treatment follow- up.	9
Liver	Primary or metastatic cancer	63	Safety of X-ray dose	Virtual unenhanced images generated from the portal venous phase could replace real non injected images and allow a reduction of x-ray dose delivered in patients undergoing assessment for malignant lesions.	10
Pancreas	Adenocarcinoma	51	Tissue characterization	Iodine-water images significantly increased the specificity for non-recurrent pancreatic tissue characterization and improved reader confidence.	11
Kidney	Focal renal lesion	136	Tissue characterization	Iodine-water images improved specificity for characterization of small (1-4 cm) renal lesions compared with conventional attenuation measurements.	12
Prostate	Prostatic carcinoma	50	Tissue characterization	Iodine-water images enabled quantitative depiction of contrast medium uptake in prostatic lesions and improved sensitivity and specificity for differentiating prostate cancer from benign prostate hyperplasia.	13
Aorta	Angiography	80	Safety of contrast material	50-60keV CT angiography with up to 60 % iodine volume load reduction provided similar image quality and accessibility than full iodine load with conventional single energy CT.	14
Musculoskeletal	Bone Metastasis	83	Lesion Detection	The combination of CT and water-hydroxyapatite images significantly increased diagnostic accuracy for detecting bone metastasis.	15
Musculoskeletal	Bone Marrow Oedema	40	Lesion Detection	Dual-energy water-hydroxyapatite images showed good diagnostic performance for bone marrow edema in patients with non-traumatic hip pain.	16
Musculoskeletal	Gout	55	Lesion Detection	The validity of GSI in gout is supported by the identification of urate in all patients with clinical gout and the good correlations with clinical characteristics.	17

Design goal of TrueFidelity for GSI

However, as in all of CT acquisitions, image noise remains a limiting factor for spectral CT when optimizing patient dose and image quality. The noise magnification is inherent and is typically more noticeable when viewing lower energy (i.e. 40-50 keV) and material selective images, due to the noisy low/high kV measurements and material decomposition process.[18] While iterative reconstruction (IR) methods have been applied to reduce the noise, the altered image texture resulted in decreased observer evaluated image quality scores, and 60 keV (or 70 keV) and color overlaid iodine map remain the images of choice by clinical readers.[19,20]

TrueFidelity for GSI was introduced in 2020 to address this challenge. Its deep neural network was specifically trained to learn the unique noise characteristics in spectral material basis (e.g., iodine and water) to reduce noise while preserving details, high iodine quantification accuracy and reader-preferred noise texture (Figure 2). The benefits apply to all image types, especially in low energy keV and material selective images.[21]

Since launch, researchers worldwide have published initial peer-reviewed evidence in well-designed phantom and clinical studies to evaluate its impact on image quality, diagnostic performance, and radiation dose optimization.

This white paper is tasked to summarize the evidence from these studies and provide reference for spectral CT users to optimize GSI protocols and improve its diagnostic value for better patient care.

TrueFidelity for GSI was specifically trained to reduce noise while preserving details, high iodine quantification accuracy and reader-preferred noise texture, for all GSI image types.[21]

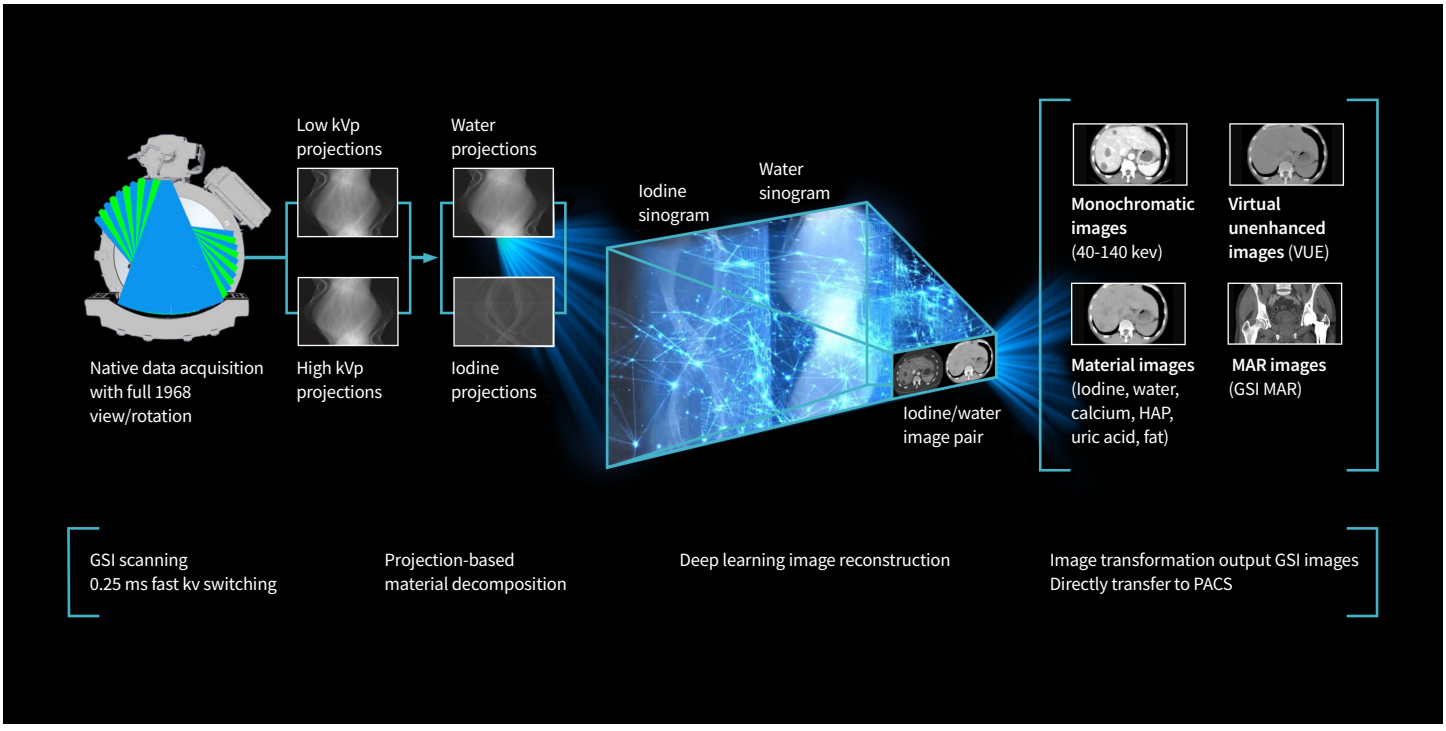

Figure 2: A schematic of TrueFidelity for GSI image generation chain. The image quality benefits are designed to apply to all GSI image types.

Evidence on improving image quality and lesion detectability

A task-based assessment of image quality led by Greffier et al. on a dual energy dedicated phantom showed that using the Medium level of TrueFidelity improved various characteristics of image quality in virtual monochromatic images ranging from 40 to 80 keV.[22] It decreased noise magnitude by an average of 27±3% compared to IR 50% across the energy range studied (Figure 3A). While images reconstructed with IR tended to have a smoother texture, the further noise reduction led by the use of TrueFidelity was associated with an improvement of the noise texture, closer to the one of Filtered Back Projection (FBP) (Figure 3B).

The lesion detectability was calculated for two types of abdominal lesions, hepatocellular carcinomas in the arterial phase and hyper vascularized metastasis. Between 40 and 80 kev, the High level of TrueFidelity increased the lesion detectability of each lesion type in average by 64% and 60% respectively (Figure 4).

TrueFidelity for GSI may increase the lesion detectability in hepatocellular carcinomas and hyper-vascular metastasis,[22] and may allow a better detection and staging of pancreatic cancer.[24]

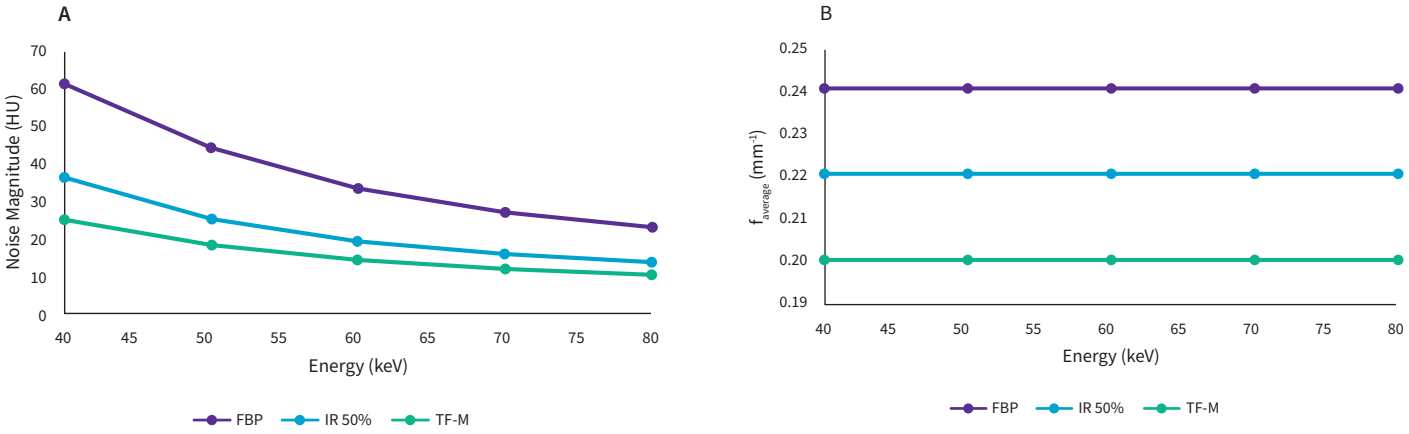

Figure 3: Impact of different CT image reconstruction algorithms on the noise magnitude and texture. Figure 3A quantifies noise magnitude measured in virtual monochromatic images of energy ranging from 40 to 80 keV and reconstructed with FBP, IR 50% and TrueFidelity at Medium level (TF-M). The results demonstrate that TrueFidelity reduces the noise magnitude in virtual monochromatic images at all energy levels. Figure 3B quantifies the noise texture of virtual monochromatic images reconstructed with FBP, IR 50% and TF-M by measuring the average spatial frequency of the noise power spectrum ($f_{average}$) as a function of energy level; the lower the average spatial frequency, the smoother the image texture. While the Noise Power Spectrum tends to be shifted to lower frequencies - resulting in a smoother texture - when using IR, images reconstructed with TrueFidelity have a noise power spectrum average frequency closer to the one of FBP leading to a more preferred image texture at all energy levels. Figure 3A and 3B were regenerated based on the published phantom results from the paper by Greffier et.al.[22] Courtesy of Joel Greffier, Ph.D, CHU de Nîmes, France.

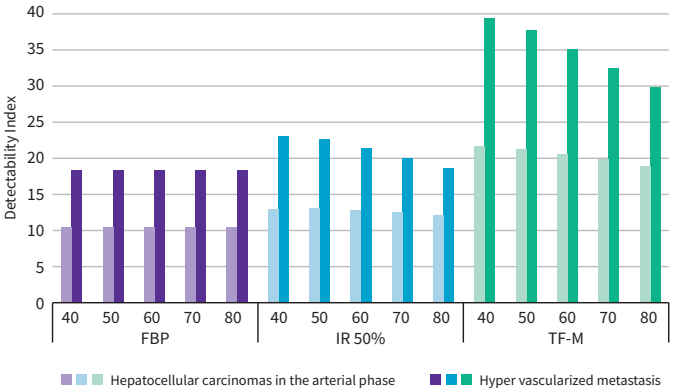

Figure 4: Impact of different CT image reconstruction algorithms on the detectability of subtle abdominal lesions. The chart was regenerated based on the phantom data published by Greffier et al.[22] They illustrate the detectability index as a function of the energy of virtual monochromatic images for FBP, IR 50%, True Fidelity at Medium level (TF-M). The detectability index is a surrogate of the radiologist's capability to detect a specific lesion type; the higher the detectability index, the easier it is to detect that given lesion. Here, the detectability index was computed for 10 mm, hepatocellular carcinomas in the arterial phase and hyper vascularized metastasis respectively. The results show that TrueFidelity Medium improves the detectability of both lesion types compared to IR 50% at all energy levels. Courtesy of Joel Greffier, Ph.D., CHU de Nîmes, France.

The work led by Noda et al. showed that the use of TrueFidelity at High Level in whole body CT angiography significantly reduced background noise and improved subjective image quality of 40 keV monochromatic images compared with IR, while maintaining the arterial depiction of almost all arteries in 22 patients.[23] Figure 5 demonstrates a clinical case where 50keV reconstructed with High level of TrueFidelity recovered the vascular contrast visualization for a patient with poor distal vascular circulation in the right leg.

Noda et al. also observed such image quality enhancement when using TrueFidelity compared to IR 40% in 30 consecutive participants with pancreatic cancer.[24] An overall improvement of signal to noise ratio in 70 keV virtual monochromatic images of the pancreas and a reduction of iodine concentration variability in material decomposition images allowed a better detection and staging of pancreatic cancer. Sato et al. assessed virtual monochromatic images of three energy levels (40-, 50-, and 70-keV) and iodine density maps of 40 patients who underwent contrast enhanced DECT of the abdomen[18]. They reported significantly lower noise in the liver, a higher CNR of the portal vein, better vessel conspicuity and overall image quality scores leading to improved lesion conspicuity scores (across 47 solid lesions rated by 2 radiologists) at all energy levels when using TrueFidelity in comparison to IR 50%.

The image quality benefits of TrueFidelity compared to IR were also qualitatively and quantitatively observed in all GSI image types (virtual monochromatic, virtual unenhanced and material decomposition) of 48 obese patients (mean body mass index = 39.5) in vascular and multiphase staging exams.[25] TrueFidelity images showed statistically significant higher Likert scores across all subjective image quality criteria rated by 4 abdominal radiologists and higher CNR and SNR in the aorta and liver compared with IR 50% (Figure 6). Figure 7 also demonstrates low-noise, high quality 65keV and material-selective iodine images reconstructed with TrueFidelity High for a BMI-39 patient with suspected pulmonary embolism.

Some preliminary studies, as the one conducted by Noda et al. in thoraco-abdomino-pelvic CT of 111 patients, showed that the image quality improvement of GSI images led by the application of TrueFidelity could offer the potential to reduce both radiation dose and contrast medium.[26]

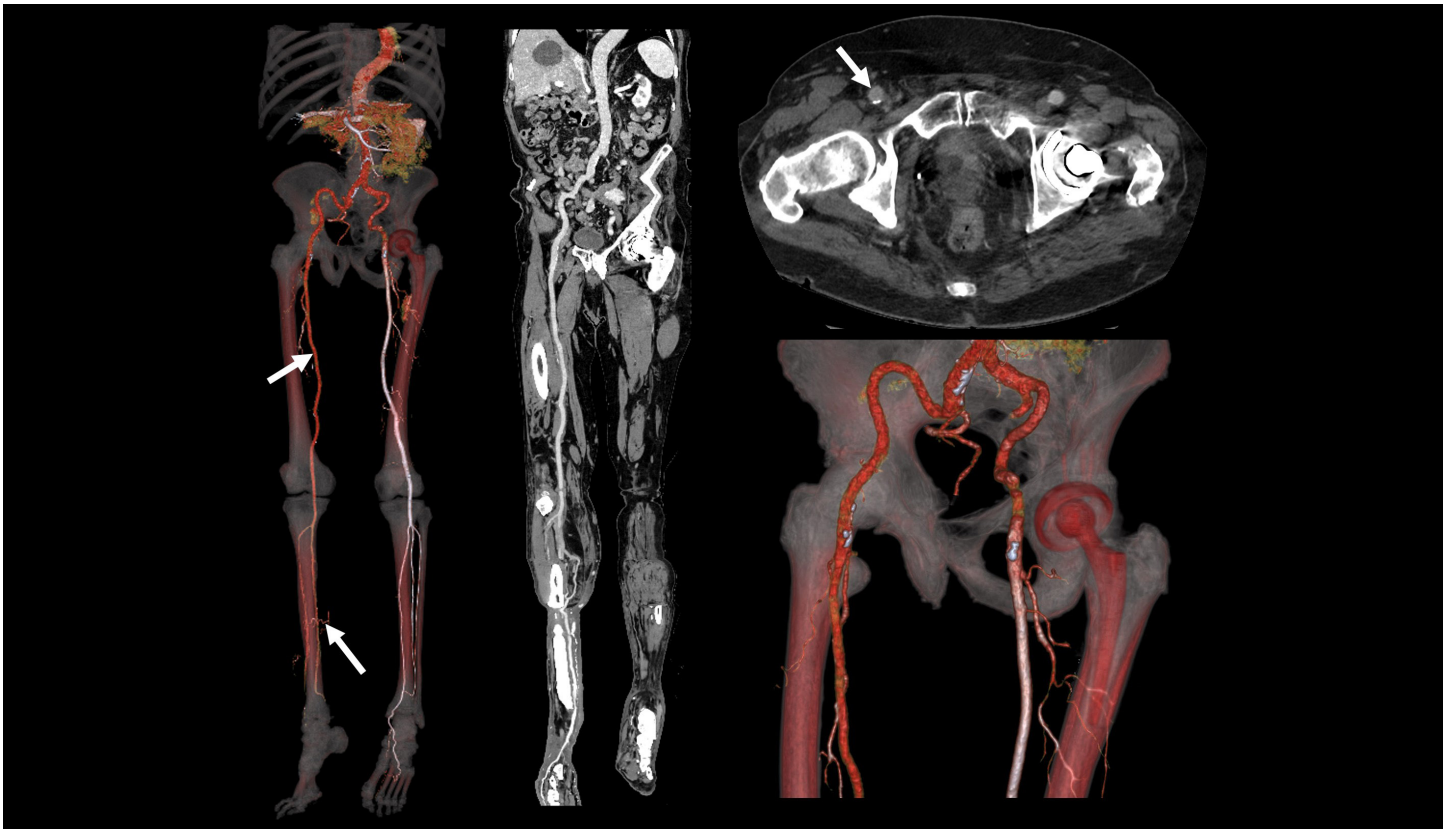

Figure 5: A patient suspicious of peripheral arterial disease received run-off spectral CT angiography, reconstructed with TrueFidelity at high level. The superb image quality of 50 keV helps recover the contrast visualization of the right distal vascular segments with the poor circulation and delayed propagation of contrast media. Courtesy of Centre Hospitalier Emile Roux, France.

Evidence on 40 keV as a potential standard for routine low-keV

Xu e t al. analyzed 30 venous phase acute abdominal DECT scans that were reconstructed with IR 60% and High Level of TrueFidelity at four different energy levels (40, 50, 74, and 100 keV).[27] TrueFidelity reduced image noise within the liver, aorta, fat, and muscle by 19.9 to 35.5% ($p < 0.001$) compared to IR in all reconstructions at identical keV levels. Subjective assessment of image noise, sharpness, texture, and overall quality performed by two board-certified radiologists demonstrated that TrueFidelity significantly improved image quality (particularly in thin sliced images) and that the ratings of 40 keV images reconstructed with TrueFidelity were of superior or equivalent to those of 50 keV reconstructed with IR. Hence, TrueFidelity may facilitate 40 keV as a new standard for routine low-keV reconstruction in contrast-enhanced abdominal DECT. Figure 8 demonstrates a clinical example of low-noise 40keV achieving high CNR and iodine conspicuity for a patient with unresectable hepatocellular carcinoma.

Noda et al. also evaluated the clinical relevance of 40 keV monochromatic images from a first group of 53 patients in comparison to 80 kVp images from a second group of 58 patients – all reconstructed with the Medium level of True Fidelity – for the diagnosis of pancreatic ductal adenocarcinoma.[28]

Compared to low-kVp polychromatic images, 40 keV monochromatic images had higher background noise but increased CT numbers of the vasculatures and parenchymal organs at both pancreatic and portal venous phases ($P < 0.001$). Due to the increased tissue enhancement, the SNR in almost all anatomical structures ($P < 0.001$-0.005) and the tumor-to-pancreas CNR ($P < 0.001$-0.01) were higher in the 40 keV group than in the 80 kVp group. This led to a better pancreatic ductal adenocarcinoma conspicuity in the 40-keV group than in the 80-kVp group ($P = 0.007$-0.03) at comparable dose length products at pancreatic (275 vs. 313 mGy*cm; $P = 0.05$) and portal venous phases (743 vs. 766 mGy*cm; $P = 0.20$).

TrueFidelity for GSI may facilitate 40 keV as a new standard for routine low-keV reconstruction in contrast-enhanced abdominal Spectral CT.[27]

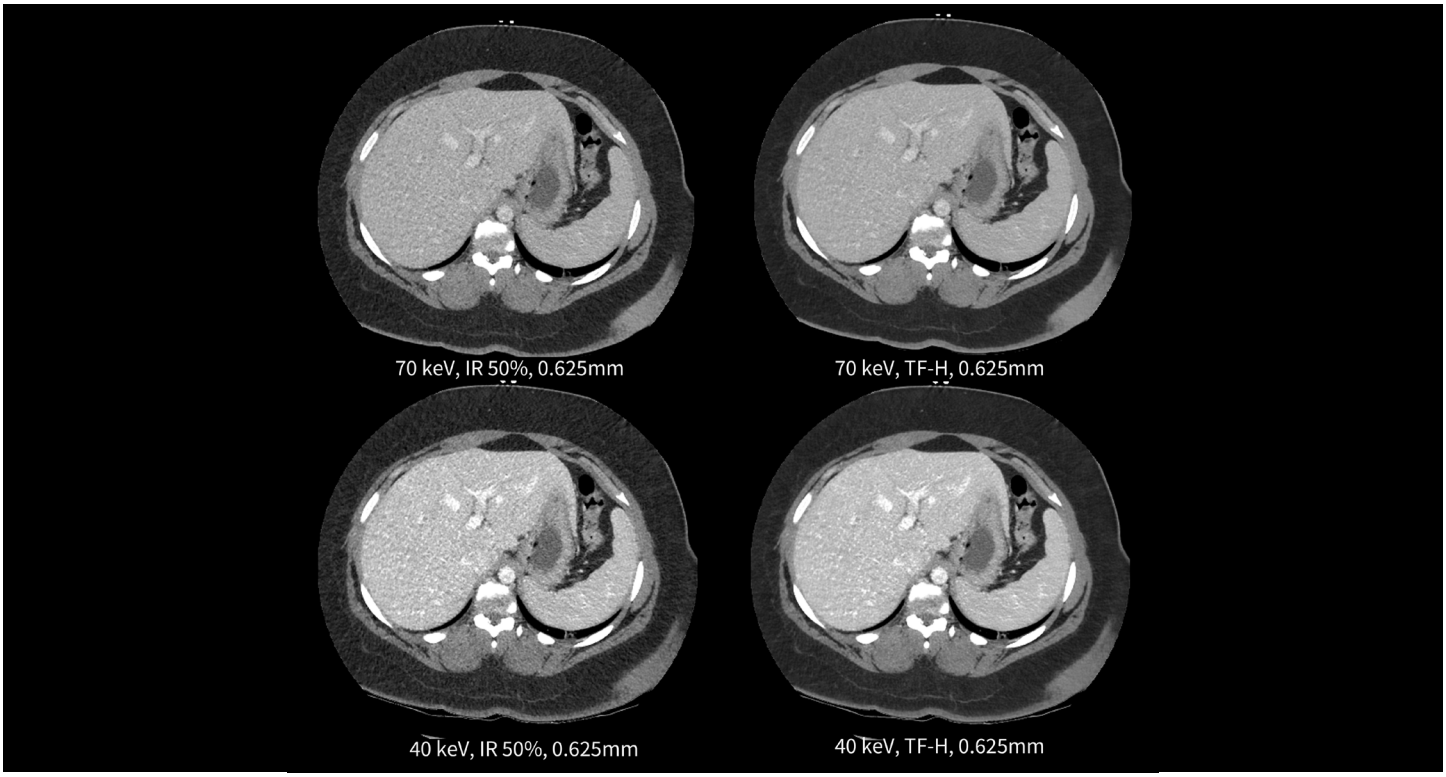

Figure 6: A BMI- 55 male with flank pain after trauma without evident injury received abdomino-pelvic spectral CT with GSI protocols, reconstructed with IR 50% and High-level of TrueFedility. TF-H demonstrate lower noise, higher image quality in both axial 40keV and 70keV. 40keV also shows higher iodine contrast compared to 70 keV. Courtesy of Froedtert Hospital, Medical College of Wisconsin, USA.

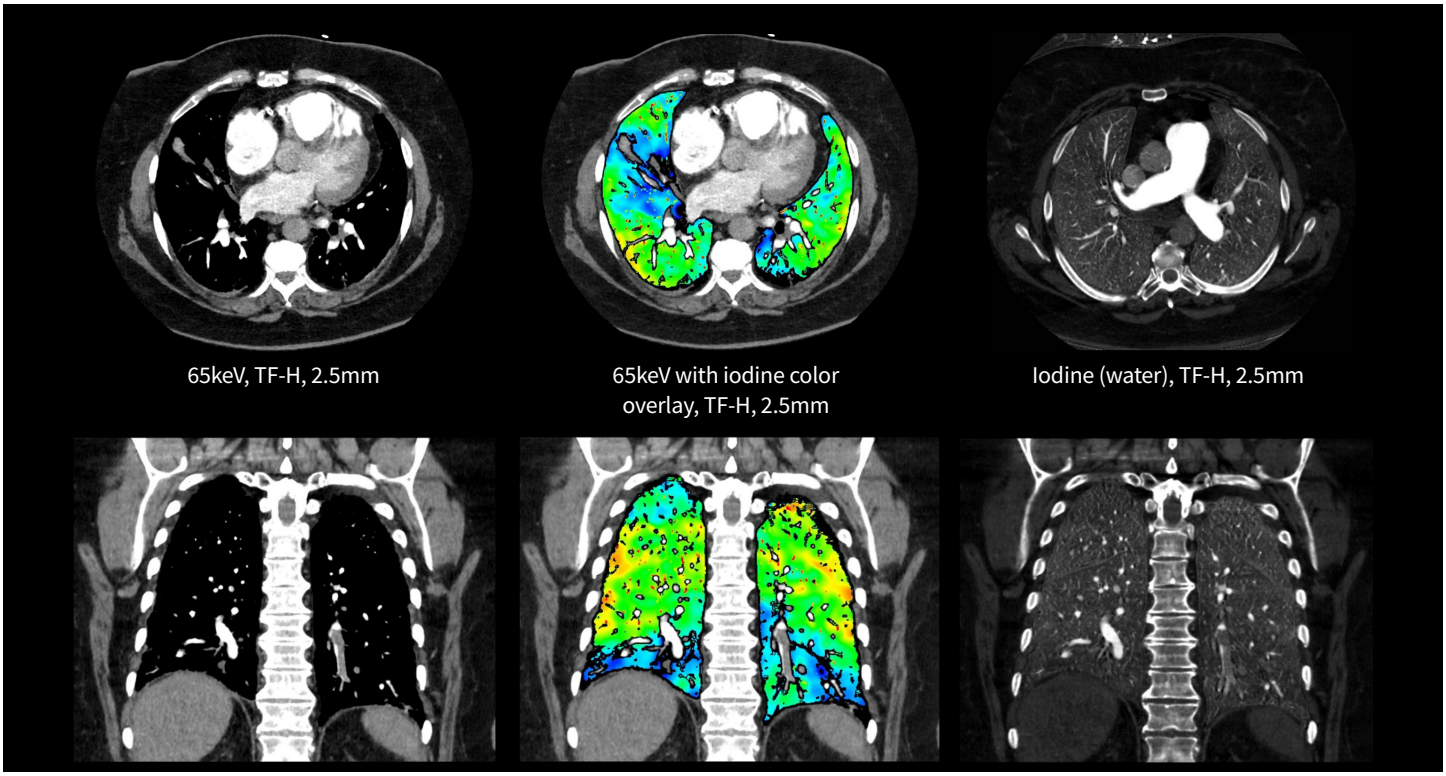

Figure 7: A BMI- 39 patient with suspected pulmonary embolism received contrast enhanced chest spectral CT scan with GSI HyperDrive fast acquisition protocol. 65 keV and Iodine images reconstructed TF-H show excellent low-noise image quality with less motion artifacts. Iodine color overlay images help highlight relative perfusion deficit areas. Courtesy of Sale Hospital, Central Gippsland Health Service, Australia.

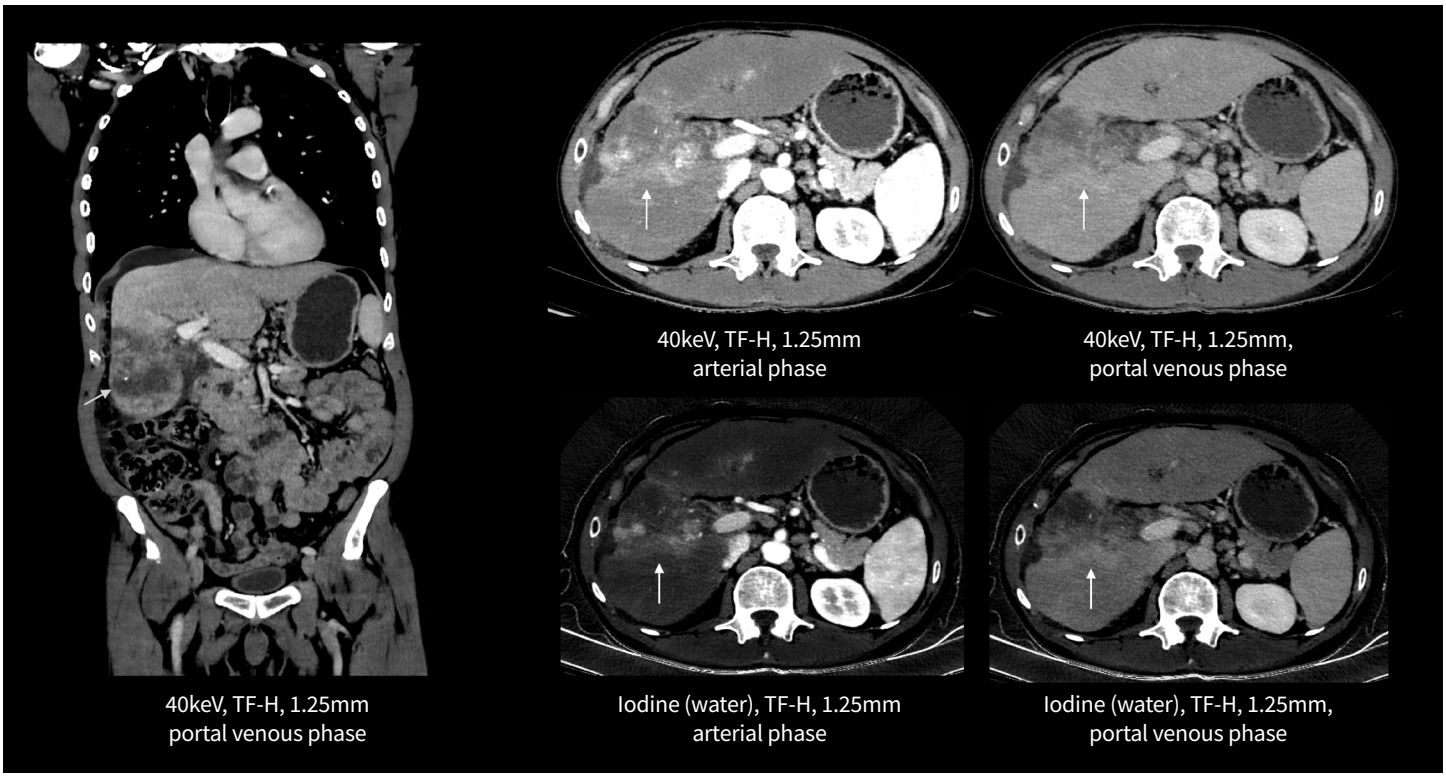

Figure 8: A patient with BMI 29 who underwent transarterial chemoembolization (TACE) for unresectable hepatocellular carcinoma (HCC). Two phases thoraco-abdomino-pelvic CT obtained with GSI protocols and 60ml contrast media. Thin slice 40keV and iodine images reconstructed with High-level of TrueFidelity demonstrate low noise, high iodine contrast-noise-ratio with clear lesion conspicuity. Courtesy of Centre Hospitalier Emile Roux, France.

Evidence on iodine quantification

While Tr ueFidelity for GSI is very effective at reducing image noise, it also succeeds at accomplishing this goal with preserving high material density quantification accuracy.

Fukutomi et al. investigated the effect of TrueFidelity compared to FBP, IR 30% and 50% on the accuracy of iodine quantification in GSI in a phantom experiment and an abdominal clinical study.[29] On the dual-energy quality control phantom containing five iodine concentrations (1, 3, 5, 8, and 12 mg/ml) and scanned at three different dose levels (CTDIvol : 9, 15, and 24 mGy), the measured iodine concentrations were equivalent among the algorithms ($p = 0.65–0.99$), and consistent with nominal values regardless of radiation dose (root-mean-square deviations of 0.08–0.36 mg/ml). Standard deviations and coefficients of variation in iodine quantification were lower on TrueFidelity images ($p<0.01$).

Similarly, in the 50 patients suspected of having focal lesions of the liver or pancreas, iodine concentrations measured in the abdominal aorta, portal vein, liver, and pancreas on both the arterial and the portal venous phases were consistent across the four reconstruction algorithms while image noise and variability of iodine concentrations were lower on TrueFidelity images ($p<0.01$).

While the measured iodine concentrations were equivalent among the different reconstruction algorithms , image noise and variability of iodine concentrations were lower on TrueFidelity for GSI images.[29]

Conclusion

The initial peer-reviewed evidence provided from both physics and clinical studies have shown that TrueFidelity for GSI is supercharging spectral CTâ€™s diagnostic performance. This is demonstrated with enhanced image quality, lesion detectability, and iodine quantification accuracy, while expanding spectral CT to patient population with high BMI. We hope that these insights will guide more CT users to adopt spectral CT in their practice.

Early evidence is based on GEHC latest 160mm-detector CT systems (i.e. Revolution CT or Revolution Apex) using small-scaled studies, limited patient demographics, and specific disease indications. The results obtained in these studies are not generalizable and may not be reproducible. Further studies designed on other GEHC CT system configurations and with larger patient cohort sizes and more robust statistical power are needed to further evaluate the benefits.

References

1. Siegel, M. J. et al. White Paper of the Society of Computed Body Tomography and Magnetic Resonance on Dual-Energy CT, Part 1: Technology and Terminology. J Comput Assist Tomogr 40, 841–845 (2016).
2. Slavic, S. et al. GSI Xtream on Revolution CTTM. Volume. Spectral. Simplified. Technology White Paper. GE HealthCare (2017).
3. Han, S. et al. Pre-treatment spectral CT combined with CT perfusion can predict hemorrhagic transformation after thrombolysis in patients with acute ischemic stroke. Eur J Radiol 156, 110543 (2022).
4. Forghani, R. et al. Low-Energy Virtual Monochromatic Dual-Energy Computed Tomography Images for the Evaluation of Head and Neck Squamous Cell Carcinoma: A Study of Tumor Visibility Compared With Single-Energy Computed Tomography and User Acceptance. J Comput Assist Tomogr 41, 565–571 (2017).
5. Wang, G., Zhang, C., Li, M., Deng, K. & Li, W. Preliminary application of high-definition computed tomographic Gemstone Spectral Imaging in lung cancer. J Comput Assist Tomogr 38, 77–81 (2014).
6. Sun, Y.-S. et al. Spectral CT imaging as a new quantitative tool? Assessment of perfusion defects of pulmonary parenchyma in patients with lung cancer. Chin J Cancer Res 25, 722–728 (2013).
7. Yunaga, H. et al. Diagnostic performance of calcification-suppressed coronary CT angiography using rapid kilovolt-switching dual-energy CT. Eur Radiol 27, 2794–2801 (2017).
8. Dubourg, B. et al. Single-source dual energy CT to assess myocardial extracellular volume fraction in aortic stenosis before transcatheter aortic valve implantation (TAVI). Diagn Interv Imaging 102, 561–570 (2021).
9. Liu, Q.-Y. et al. Application of gemstone spectral imaging for efficacy evaluation in hepatocellular carcinoma after transarterial chemoembolization. World J Gastroenterol 22, 3242–3251 (2016).
10. Lacroix, M. et al. Virtual unenhanced imaging of the liver derived from 160-mm rapid-switching dual-energy CT (rsDECT): Comparison of the accuracy of attenuation values and solid liver lesion conspicuity with native unenhanced images. Eur J Radiol 133, 109387 (2020).
11. Parakh, A., Patino, M., Muenzel, D., Kambadakone, A. & Sahani, D. V. Role of rapid kV-switching dual-energy CT in assessment of post-surgical local recurrence of pancreatic adenocarcinoma. Abdom Radiol (NY) 43, 497–504 (2018).
12. Marin, D. et al. Characterization of Small Focal Renal Lesions: Diagnostic Accuracy with Single-Phase Contrast-enhanced Dual-Energy CT with Material Attenuation Analysis Compared with Conventional Attenuation Measurements. Radiology 284, 737–747 (2017).
13. Zhang, X. F. et al. Quantitative iodine-based material decomposition images with spectral CT imaging for differentiating prostatic carcinoma from benign prostatic hyperplasia. Acad Radiol 20, 947–956 (2013).
14. Carrascosa, P. et al. Substantial iodine volume load reduction in CT angiography with dual-energy imaging: insights from a pilot randomized study. Int J Cardiovasc Imaging 30, 1613–1620 (2014).
15. Ishiwata, Y. et al. Improved Diagnostic Accuracy of Bone Metastasis Detection by Water-HAP Associated to Non-contrast CT. Diagnostics (Basel) 10, 853 (2020).
16. Son, W., Park, C., Jeong, H. S., Song, Y. S. & Lee, I. S. Bone marrow edema in non-traumatic hip: high accuracy of dual-energy CT with water-hydroxyapatite decomposition imaging. Eur Radiol 30, 2191–2198 (2020).
17. Svensson, E. et al. Dual energy CT findings in gout with rapid kilovoltage-switching source with gemstone scintillator detector. BMC Rheumatol 4, 7 (2020).
18. Sato, M. et al. Deep learning image reconstruction for improving image quality of contrast-enhanced dual-energy CT in abdomen. Eur Radiol 32, 5499–5507 (2022).
19. Chen, L.-H. et al. Image quality comparison of two adaptive statistical iterative reconstruction (ASiR, ASiR-V) algorithms and filtered back projection in routine liver CT. Br J Radiol 91, 20170655 (2018).
20. Ren, Z. et al. Application of Adaptive Statistical Iterative Reconstruction-V With Combination of 80 kV for Reducing Radiation Dose and Improving Image Quality in Renal Computed Tomography Angiography for Slim Patients. Acad Radiol 26, e324–e332 (2019).
21. Thibault, J.-B., Nett, B., Tang, J. & Liu, E. TrueFidelityTM for GemstoneTM Spectral Imaging. A new generation of spectral imaging powered by deep learning. Technical white paper on deep learning image reconstruction for spectral imaging. GE HealthCare (2021).
22. Greffier, J. et al. Phantom task-based image quality assessment of three generations of rapid kV-switching dual-energy CT systems on virtual monoenergetic images. Medical Physics 49, 2233–2244 (2022).
23. Noda, Y. et al. Deep-learning image-reconstruction algorithm for dual-energy CT angiography with reduced iodine dose: preliminary results. Clin Radiol 77, e138–e146 (2022).
24. Noda, Y. et al. Deep learning image reconstruction algorithm for pancreatic protocol dual-energy computed tomography: image quality and quantification of iodine concentration. Eur Radiol 32, 384–394 (2022).
25. Fair, E. et al. Image Quality Evaluation in Dual-Energy CT of the Chest, Abdomen, and Pelvis in Obese Patients With Deep Learning Image Reconstruction. J Comput Assist Tomogr (2022) doi:10.1097/RCT.0000000000001316.
26. Noda, Y. et al. Radiation and iodine dose reduced thoraco-abdomino-pelvic dual-energy CT at 40 keV reconstructed with deep learning image reconstruction. Br J Radiol 95, 20211163 (2022).
27. Xu, J. J., Lönn, L., Budtz-Jørgensen, E., Hansen, K. L. & Ulriksen, P. S. Quantitative and qualitative assessments of deep learning image reconstruction in low-keV virtual monoenergetic dual-energy CT. Eur Radiol 32, 7098–7107 (2022).
28. Noda, Y. et al. Comparison of image quality and pancreatic ductal adenocarcinoma conspicuity between the low-kVp and dual-energy CT reconstructed with deep-learning image reconstruction algorithm. Eur J Radiol 159, 110685 (2022).
29. Fukutomi, A. et al. Deep learning image reconstruction to improve accuracy of iodine quantification and image quality in dual-energy CT of the abdomen: a phantom and clinical study. Eur Radiol (2022) doi:10.1007/s00330-022-09127-1.

August 2023

JB23533XX

GE HealthCare